Synthesis and Characterization of Ferroferriborate (Fe₃BO₅) Nanorods

By *Yi Liu, Sheng Peng, Yong Ding, Chuanbing Rong, Jaemin Kim, J. Ping Liu, Zhong Lin Wang,* and *Shouheng Sun**

Fe₃BO₅ nanorods with diameters from 4 nm to 16 nm and length from 43 nm to 60 nm are synthesized by a facile thermal decomposition of iron acetylacetonate and *t*-butylamine borane (TBAB). TBAB is used to control the 1D growth and the aspect ratio of the nanorods. These Fe₃BO₅ nanorods are antiferromagnetic with $T_N = 174$ K, which is higher than that of bulk Fe₃BO₅ (114 K).

1. Introduction

Ferroferriborate (Fe₃BO₅) naturally exists as a mineral, vonsenite, which belongs to the family of ludwigites. It has the chemical formula 2MO•M′BO₃, where M and M′ are divalent and trivalent 3d metal ions, and an orthorhombic crystal structure with space group *pbam*.[1–4] As a mixed valence compound, ferroferriborate shows a number of interesting properties, including its catalytic oxidation of ethyl acetate and methanol[5–6] and its paramagnetic–antiferromagnetic transition at 114 K.[1–2] In addition, this material has a charge ordering crossover at ∼220 K, as demonstrated in electrical resistance measurements[1–2] and specific heat measurements.[4] Bulk Fe₃BO₅ is synthesized by solid-state thermal reaction of a stoichiometric mixture of iron oxide, metallic Fe and B₂O₃. The reaction usually takes place in sealed evacuated containers at high temperatures (823 °C to 1 120 °C) for hours (5 h to 3 days).[1,4–5] Nanoscale Fe₃BO₅ is rarely reported thus far except for ∼250 × ∼10 μm plywood-like Fe₃BO₅ nanorods made using a hydrothermal method,[7] and Fe₃BO₅ and GdBO₃ particles produced from interface diffusion between Fe–Gd particle cores and B₂O₃/H₃BO₃ shells.[8]

Here we report the synthesis of Fe₃BO₅ nanorods with tunable aspect ratio by a facile solution-phase reaction. We demonstrated recently that monodisperse Fe₃O₄ nanoparticles were readily synthesized via reductive decomposing of iron acetylacetonate (Fe(acac)₃) in the presence of 1,2-hydrocarbondiol, oleic acid (OA), and oleylamine (OAm).[9] We further noticed that *t*-butylamine borane (TBAB) could be used as a weak reducing agent for producing Au and Pd nanoparticles in the presence of oleylamine.[10–11] Reasoning that TBAB might offer a reliable source of boron, we replaced 1,2-hydrocarbondiol with TBAB during the synthesis of Fe₃O₄ nanoparticles and succeeded in synthesizing Fe₃BO₅ nanorods. The as-synthesized Fe₃BO₅ nanorods were not thermally stable, as thermal annealing at 500 °C converted the rod to sphere-like morphology with serious particle sintering. However, these nanorods could be stabilized by SiO₂ coating. We found that SiO₂-coated Fe₃BO₅ nanorods were thermally stable under an Ar atmosphere. Upon reductive annealing up to 700 °C under a gas mixture of 95% Ar and 5% H₂, small Fe nanoparticles evolved from the major Fe₃BO₅ phase. Our synthesis offers a convenient route to nanostructured Fe₃BO₅ with anisotropic shapes that is interesting for magnetic and catalytic studies.

2. Nanorod Synthesis

2.1. Synthesis of Fe₃BO₅ Nanorods

The Fe₃BO₅ nanorods were synthesized by a high-temperature reaction between Fe(acac)₃ and TBAB in a mixture solvent of OA and OAm. With 2 mmol Fe(acac)₃ dissolved in 4 mL OA and 13 mL OAm at 180 °C followed by injection of 1 mmol TBAB in 3 mL OAm solution and heating at 300 °C, Fe₃BO₅ nanorods were obtained. Spherical Fe₃O₄ nanoparticles were also found in the final product and were removed from the nanorod product by controlled precipitation of nanorods and centrifugation (3 500 rpm) from which Fe₃BO₅ nanorods were precipitated out while the Fe₃O₄ nanoparticles suspended in the supernatant were discarded. After this size-selective precipitation, high quality 5 × 45 nm Fe₃BO₅ nanorods were separated. Figure 1a is a representative transmission electron microscopy (TEM) image of the nanorods obtained. The as-synthesized Fe₃BO₅ nanorods were dispersed in hexane and were stable in hexane for over 10 months at ambient conditions without noticeable agglomeration.

Addition of TBAB was the key to preparing Fe₃BO₅ nanorods in the current synthetic condition. TBAB has been used as a reducing

[*] Prof. S. Sun, Y. Liu, Dr. S. Peng, Dr. J. Kim
     Department of Chemistry
     Brown University
     Providence, Rhode Island 02912 (USA)
     E-mail: ssun@brown.edu
     Dr. Y. Ding, Prof. Z. L. Wang
     School of Materials Science and Engineering
     Georgia Institute of Technology
     Atlanta, Georgia 30332 (USA)
     Dr. C. Rong, Prof. J. Ping Liu
     Department of Physics
     University of Texas at Arlington
     Arlington, Texas 76019 (USA)

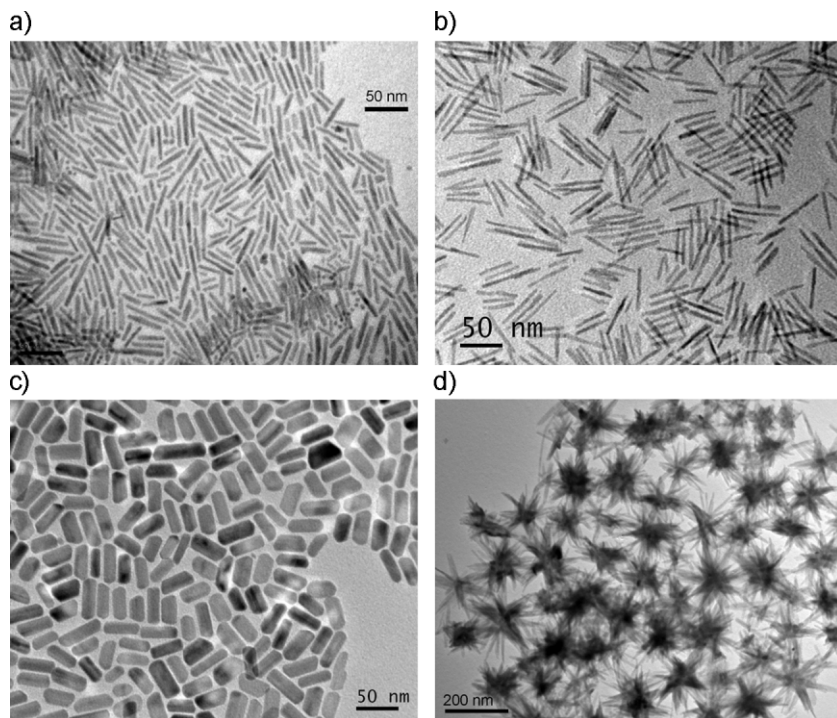**Final page numbers not assigned**

Figure 1. TEM images of the as-synthesized a) 5×45-nm, b) 4×60-nm, and c) 16×43-nm Fe_3BO_5 nanorods, and d) 150-nm nanospikes.

agent in the syntheses of intermetallic PtPb nanorods and gold nanoparticles.[12–13] It is believed that TBAB has a mild reducing power compared with the commonly used reducing agents such as $NaBH_4$ and $LiBH(C_2H_5)_3$, which facilitates the controlled growth of nanoparticles. In our synthesis, TBAB not only functioned as a reducing agent but also provided boron. The aspect ratio of the Fe_3BO_5 nanorods was tuned by varying the TBAB amount. As TBAB usage was increased from 1 mmol to 1.2 mmol, the Fe_3BO_5 nanorods were changed from 5×45 nm (Fig. 1a) to 4×60 nm (Fig. 1b). When TBAB was reduced from 1 mmol to 0.8 mmol, wider rods (16×43 nm) were produced (Fig. 1c). Further reduction of TBAB to 0.6 mmol led to insufficient 1D growth and the formation of spherical Fe_3O_4 as a major product (Fig. S1 of the Supporting Information). In contrast, when a large amount of TBAB (1.5 mmol) was added, the extra TBAB facilitated the multiple 1D growth around one nanostructure, giving flower-like hyper-branched nanospikes with diameters around 150 nm (Fig. 1d). However, these nanospikes were not stable in hexane and were precipitated out in a few hours.

2.2. Characterization of Fe_3BO_5 Nanorods

The structure of Fe_3BO_5 nanorods was studied by high resolution transmission electron microscopy (HRTEM). From a representative HRTEM of a 5×45 nm Fe_3BO_5 nanorod (Fig. 2a), the crystal lattice fringes have distances of 3.04 Å and 4.64 Å, which correspond to the interplanar spacings of (001) and (200) planes. This indicates that the growth of nanorod is along the [001] direction, the c axis of the Fe_3BO_5 crystal. In the HRTEM image of a

16×43-nm Fe_3BO_5 nanorod (Fig. 2b), the same growth direction is observed and the growth is terminated by {201} planes. This is consistent with what is reported in the formation of the plywood-like Fe_3BO_5 nanorods.[7] The a–c plane views of the nanorods shown in Figure 2a and b seem to indicate that the nanorods are in single crystal structures. However, multiple views of a 16×43 nm Fe_3BO_5 nanorod from different directions reveal the polycrystalline nature of the nanorod (Fig. 2c and d). In Figure 2c, two crystal domains are seen and the twin plane with a darker contrast is marked by white arrows. Figure 2d is a cross-section view of the rod along its c direction. The five-fold-twin structure is clearly visible.

Inductively coupled plasma atomic emission spectroscopy (ICP-AES) was used to measure the elemental compositions of the Fe_3BO_5 nanorods prepared with different TBAB injection. For typical Fe_3BO_5 nanorods, as shown in Figure 1a, the atomic ratio of Fe:B was 73.9:26.1 which was close to 3:1 in the molecular formula. For the wider Fe_3BO_5 nanorods shown in Figure 1c, the Fe:B ratio was detected to be 76.0:24.0, still close to 3:1, although the rods were slightly Fe rich.

X-ray diffraction (XRD) patterns were used to characterize the crystal structure of the Fe_3BO_5 nanorods. The XRD pattern of the as-synthesized Fe_3BO_5 nanorods (Fig. 3a) shows broad peaks, indicating the presence of small crystalline domains within each nanorod structure. To further characterize the structure, we annealed the 5×45-nm nanorods in argon. At 600 °C or below, the structure did not crystallize well. But at 700 °C for 1 h, the polycrystalline structure was converted into single crystal as indicated by the narrow diffraction peaks of Fe_3BO_5 in the XRD pattern (Fig. 3b). The 16×43-nm Fe_3BO_5 nanorods annealed under these same conditions also gave Fe_3BO_5 but a small amount of bcc-Fe was also seen in the diffraction pattern (Fig. 3c and d). The single crystalline diffraction peaks from the annealed Fe_3BO_5 nanorods match well with the standard pattern of orthorhombic Fe_3BO_5 with space group *pbam* [55] and $a = 9.463$ Å, $b = 12.305$ Å, $c = 3.073$ Å (Fig. 3e). The narrow XRD peaks further indicate that the Fe_3BO_5 nanorods cannot survive the high-temperature annealing conditions; they tend to coalesce into larger single crystals. This is easily understood considering that {100} surfaces are not thermodynamically favorable in the twinned nanorod structure and should be reduced at high temperatures.

2.3. Proposed Growth Mechanism

The growth mechanism of the Fe_3BO_5 nanorods has not been fully investigated. But our initial experimental results indicated that polyhedral Fe_3O_4 nuclei were formed at 180 °C before the injection of TBAB. The injection of TBAB initiated the growth of Fe_3BO_5 onto the Fe_3O_4 nuclei. The pentagonal nanorod shown in Figure 2d might evolve from the energy preferred 5-fold-twinned
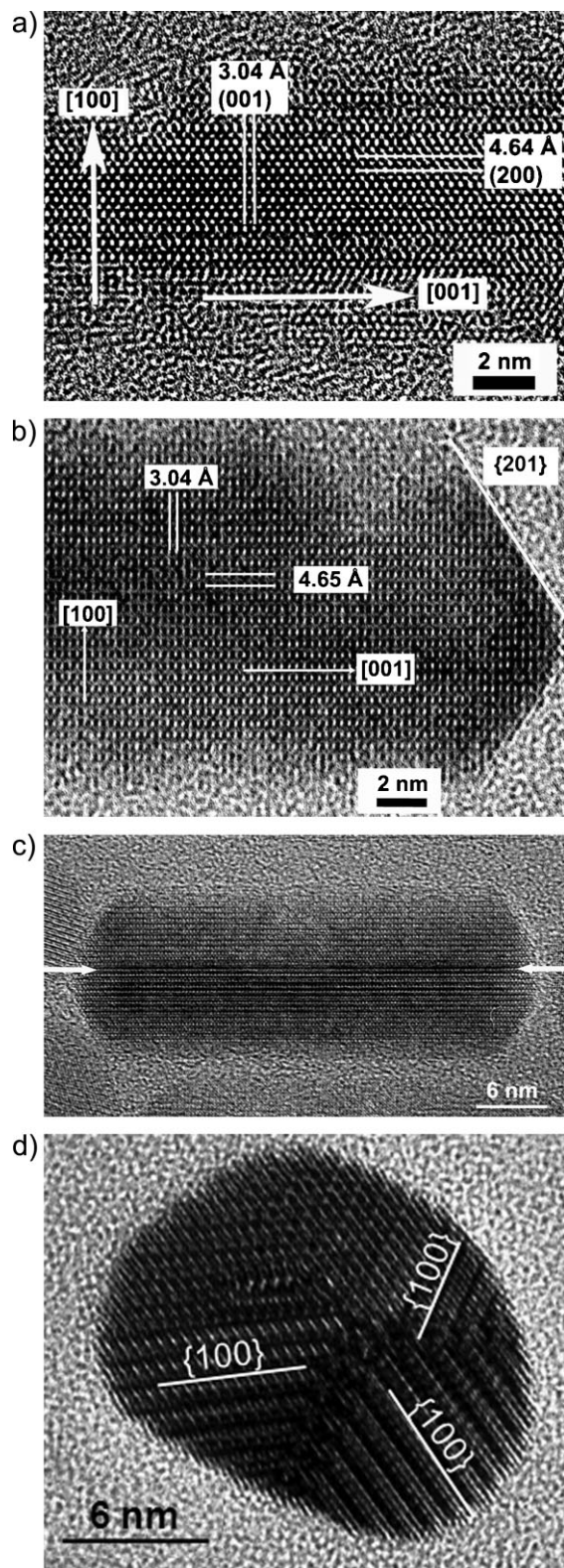
2

© 2009 WILEY-VCH Verlag GmbH & Co. KGaA, Weinheim

Adv. Funct. Mater. **2009**, *19*, 1–5

Final page numbers not assigned

Figure 2. HRTEM images of a) a 5 × 45-nm Fe₃BO₅ nanorod (a–c plane view), b) a 16 × 43-nm Fe₃BO₅ rod (a–c plane view), c) a 16 × 43-nm Fe₃BO₅ nanorod with two visible crystal domains shown within the rod (a–c plane view), and d) a 16 × 43-nm Fe₃BO₅ nanorod with five crystal domains visible (view from the *c* direction).
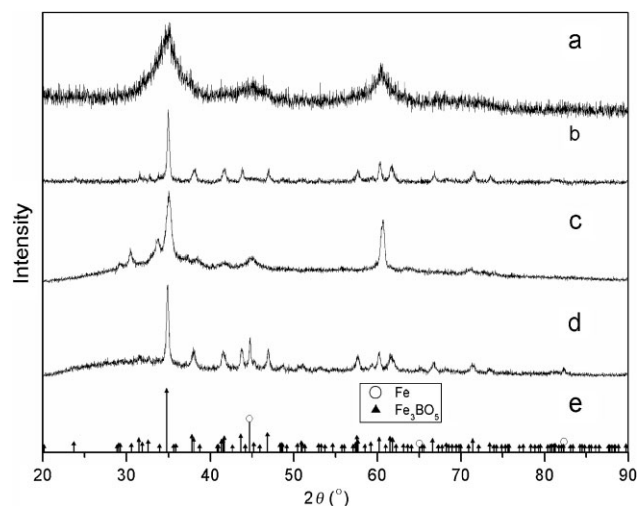

Figure 3. XRD diffraction patterns of a) the as-synthesized 5 × 45-nm Fe₃BO₅ nanorods, b) the 5 × 45-nm Fe₃BO₅ nanorods annealed in argon at 700 °C for 1 h, c) the as synthesized 16 × 43-nm Fe₃BO₅ nanorods, d) the 16 × 43-nm Fe₃BO₅ nanorods annealed in argon at 700 °C for 1 h, and e) the standard bcc-Fe (Powder Diffraction File 00-006-0696) and orthorhombic synthetic vonsenite Fe₃BO₅ (Powder Diffraction File 01-075-1659).

decahedron structure and the [001] growth might be due to the preferential binding of OA and OAm to the {010} facets and the preferential crystallization of Fe₃BO₅ on the {201} facets at the tips of nanorods (Fig. 2b). A similar growth mechanism has been observed in the syntheses of nanorods of Ag[14] and Pd.[15] We found that when the TBAB was injected at higher temperature (at 300 °C for example), the product was mostly polyhedral Fe₃O₄ nanoparticles and Fe₃BO₅ was difficult to be detected. This is because at 300 °C, the Fe₃O₄ nuclei might already grow into large particles on which 1D growth could not be initiated and/or the decomposition of TBAB was too fast for B to be doped into iron oxide matrix.

2.4. Reductive Annealing of Fe₃BO₅ Nanorods

Fe₃BO₅ nanorods can be reduced in a mild reducing atmosphere to form bcc-Fe and B-based oxide. For example, the 5 × 45-nm nanorods annealed under a gas mixture of 5% H₂ and 95% argon at 500 °C for 1 h gave spherical single-crystalline bcc-Fe particles, as shown by TEM (Fig. S2 of the Supporting Information). Boron-related species were difficult to characterize due to the presence of amorphous boron oxides. To protect the nanorod from coalescence, we coated the Fe₃BO₅ nanorods with 10-nm silica following a literature method.[16] Figure 4a is a TEM image of the 5 × 45-nm Fe₃BO₅ nanorods coated with a ~10-nm-thick SiO₂ shell. With the silica coating, the shape of the Fe₃BO₅ nanorods was well-protected during annealing either under argon (Fig. S3 of the Supporting Information) or under a gas mixture of 5% H₂ and 95% argon at 700 °C for 1 h (Fig. 4b). Selected-area electron-diffraction (SAED) patterns of the as-synthesized Fe₃BO₅ nanorods, Fe₃BO₅/SiO₂ nanorods, and the annealed Fe₃BO₅/SiO₂ nanorods are shown in Figure S4 of the Supporting Information. There is no obvious
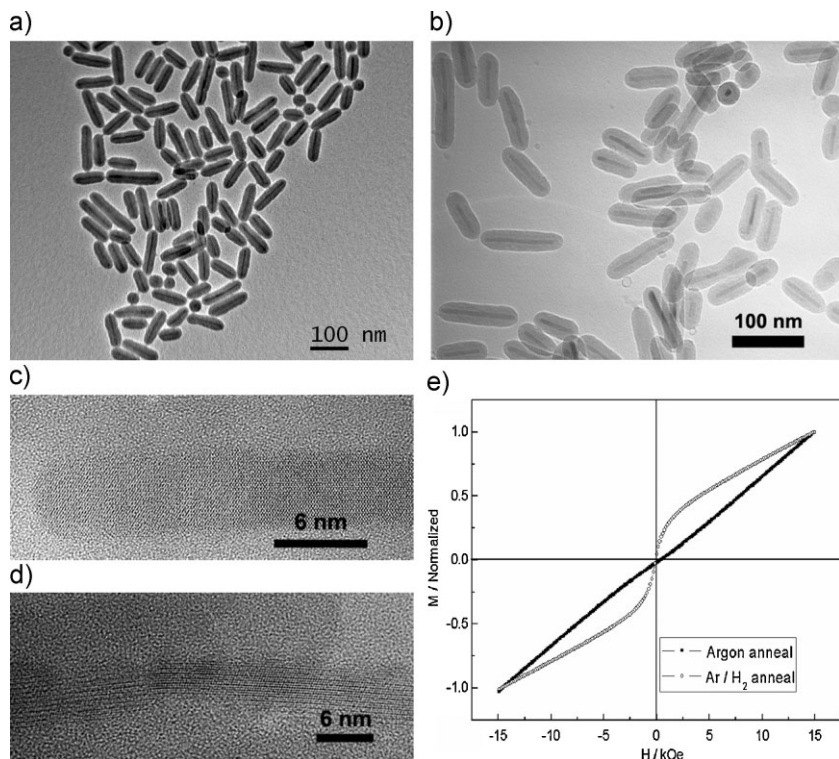
Final page numbers not assigned

Figure 4. TEM images of a) silica-coated Fe_3BO_5 nanorods, b) silica-coated Fe_3BO_5 nanorods annealed in Ar/H_2 at 700 °C for 1 h. HRTEM images of a single silica-coated Fe_3BO_5 nanorod annealed c) in argon at 700 °C for 1h and d) in Ar/H_2 at 700 °C for 1 h. e) Room-temperature magnetic hysteresis loops of Fe_3BO_5/SiO_2 nanorods annealed in argon and in Ar/H_2.

antiferromagnetic nanoparticles of Co_3O_4[17] and CuO.[18] The magnetic behavior of the Fe_3BO_5 nanorods was further studied by temperature-dependent magnetic susceptibility measurements. Figure 5b shows that zero-field-cooling (ZFC) and field-cooling (FC) curves measured at a 1 kOe applied field. The plots of the inverse susceptibility ($1/\chi_g$) as a function of temperature (inset of Fig. 5b) show a deviation from the linear dependence below 174 K. This change marks the Néel temperature (T_N) at 174 K. For bulk Fe_3BO_5, the T_N was reported to be 114 K[1], and T_N of the plywood-like Fe_3BO_5 nanorods was 140 K[7]. Our Fe_3BO_5 nanorods show a further increased T_N. The ZFC and FC susceptibility curves are essentially the same above 115 K. The ZFC curve reaches a maximum at 76 K. Below 76 K, as temperature decreases, χ_g decreases in ZFC curve and increases in FC curve. This splitting between ZFC and FC curves as temperature decreases has been reported on antiferromagnetic NiO nanoparticles [19] and α-Fe_2O_3 nanowires.[20] These may be explained by what has been proposed by Néel and co-workers. As particle size decreases to only a few nanometers, the uncompensated magnetic spins associated with the surface atoms become significant and give rise to a net magnetization.[21]

diffraction pattern change, indicating the major crystal phase in the nanorod structure is still Fe_3BO_5. This is confirmed by HRTEM of the coated rods annealed in argon (Fig. 4c). But the nanorods annealed under the gas mixture of Ar and H_2 exhibit numerous darker particle domains (Fig. 4d). Comparing with the room-temperature magnetic hysteresis loops of the Fe_3BO_5/SiO_2 nanorods annealed under argon, which are paramagnetic, and those annealed under Ar/H_2, which show superparamagnetic behavior (Fig. 4e), as well as the formation of bcc-Fe upon reductive annealing of Fe_3BO_5 (Fig. S2 of the Supporting Information), we can assume that such dark spots are Fe grains. The conclusion is that a 10-nm silica coating can not only protect the Fe_3BO_5 nanorod shape under reductive annealing conditions, but also prevent the small Fe domains formed during the annealing from coalescence within the rod structure.

2.5. Magnetic Properties of Fe_3BO_5 Nanorods

The Fe_3BO_5 nanorods show interesting magnetic properties. For the 5×45-nm Fe_3BO_5 nanorods, their room temperature hysteresis loop is linearly M-H dependent, which is typical of paramagnetic materials (Fig. 4e, and Fig. S5 of the Supporting Information). But at 5 K, they have an open hysteresis with a coercivity field of 1 009 Oe and a remanence of 0.078 emu g^{-1} (Fig. 5a). Similar open hysteresis loops have been observed in other

3. Conclusions

In summary, we have developed a facile solution-phase synthesis of Fe_3BO_5 nanorods by reductive thermal decomposition of $Fe(acac)_3$ in the presence of t-butylamine borane. The aspect ratios of the Fe_3BO_5 nanorods can be controlled by the amount of t-butylamine borane used in the synthesis. These nanorods are antiferromagnetic at 174 K or below but are paramagnetic at above 174 K. Upon the coating with a layer of SiO_2, the morphology of the nanorods is well-preserved even at 700 °C annealing conditions and Fe_3BO_5 can be converted to bcc-Fe and boron oxides when annealed under a reducing atmosphere (95% Ar and 5% H_2). This synthesis offers a new Fe_3BO_5 nanoscale platform for further study of the physical and chemical properties of this class of materials.

4. Experimental

t-Butylamine borane (97%), oleic acid (90%), oleylamine (80–90%), $Nd(acac)_3$, IGEPAL CO-520, and tetraethyl orthosilicate (>99.0%) were purchased from Aldrich. $Fe(acac)_3$ (99%) was purchased from Strem. All chemicals were used without further purification.

Synthesis of Fe_3BO_5 Nanorods: 2 mmol $Fe(acac)_3$ was mixed with 4 mL oleic acid and 13 mL oleylamine. Under a nitrogen flow the mixture was first heated to 120 °C for 1 h. Then the mixture was heated to 180 °C and kept at this temperature for 45 min. Subsequently, 1 mmol t-butylamine borane in 3 mL oleylamine solution was injected into the solution and the reaction mixture was kept at 180 °C for another 15 min before it was heated to
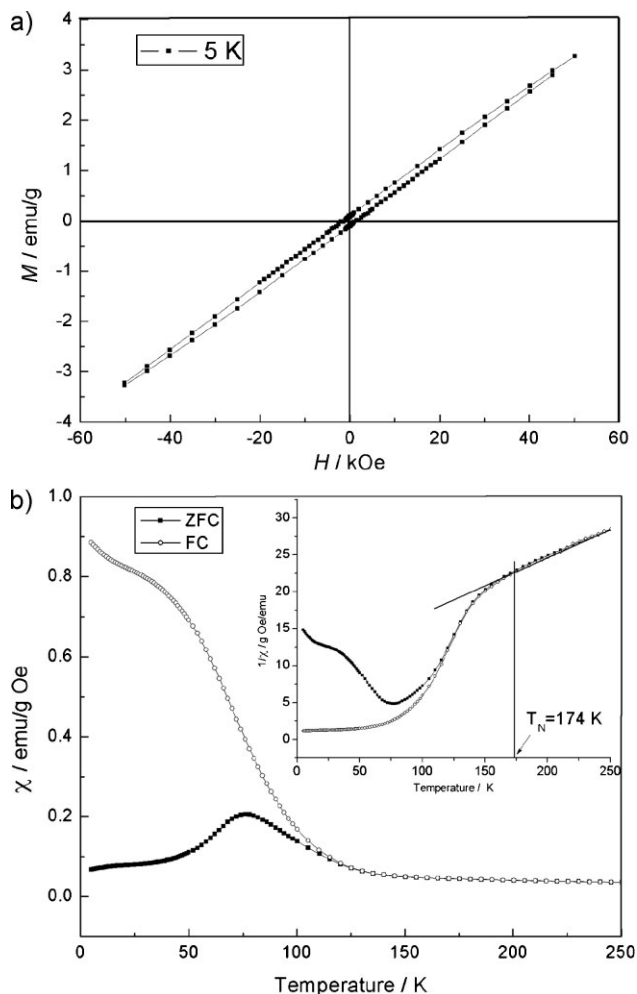
Final page numbers not assigned

Figure 5. a) Magnetic hysteresis loops of 5×45-nm Fe_3BO_5 nanorods at 5 K. b) Magnetic susceptibility versus temperature (χ_g vs. T) in ZFC and FC modes of 5×45-nm Fe_3BO_5 nanorods. Inset: $1/\chi_g$ versus T curves.

The reaction flask was sealed with a septa rubber and magnetically stirred at room temperature for 48 h. The silica-coated nanorods were precipitated out by adding 20 mL methanol. The precipitate was washed twice with a mixture of 20 mL ethanol and 25 mL hexane. The Fe_3BO_5/SiO_2 nanorods were dispersed in ethanol.

Characterization: The size and morphology of the nanoparticles were characterized by a Philips EM 420 (120 kV), a JEOL 2010, and a JEOL 4000 EX transmission electron microscope. X-ray powder diffraction patterns of the samples were recorded on a Bruker AXS D8-Advanced diffractometer with Cu Kα radiation ($\lambda = 1.5418$ Å). Magnetic studies were performed on a superconducting quantum interface device (SQUID) with a field up to 70 kOe and a vibrating sample magnetometer (VSM) with a field up to 1.55 kOe. The compositions of the samples were characterized by inductively coupled plasma atomic emission spectroscopy (ICP-AES).

Acknowledgements

[1] A. P. Douvalis, A. Moukarika, T. Bakas, G. Kallias, V. Papaefthymiou, *J. Phys.: Condens. Matter* **2002**, *14*, 3303.
[2] R. B. Guimarães, M. Mir, J. C. Fernandes, M. A. Continentino, *Phys. Rev. B: Condens. Matter Mater. Phys.* **1999**, *60*, 6617.
[3] J. C. Fernandes, R. B. Guimarães, M. A. Continentino, L. Ghivelder, R. S. Freitas, *Phys. Rev. B: Condens. Matter Mater. Phys.* **2000**, *61*, R850.
[4] M. Mir, R. B. Guimarães, J. C. Fernandes, M. A. Continentino, A. C. Doriguetto, Y. P. Mascarenhas, J. Ellena, E. E. Castellano, R. S. Freitas, L. Ghivelder, *Phys. Rev. Lett.* **2001**, *87*, 147201(1-4).
[5] Z. Cherkezova-Zheleva, T. Tsoncheva, G. Tyuliev, I. Mitov, *Appl. Catal, A* **2006**, *298*, 24.
[6] I. Mitov, D. Dotcheva, Z. Cherkezova-Zheleva, V. Mitrov, In *Metal-Ligand Interactions in Chemistry, Physics and Biology*, *NATO Sci. Series C*, (Eds: N. Russo, D. R. Salahub), Kluwer Academic Publishers, Dordrecht **2000**, vol. *546*, p. 383.
[7] H. Qi, Q. Chen, *Chem. Lett.* **2008**, *37*, 752.
[8] P. Z. Si, E. Brück, Z. D. Zhang, O. Tegus, K. H. J. Buschow, W. S. Zhang, J. C. P. Klaasse, F. R. de Boer, *Phys. B* **2004**, *353*, 1.
[9] S. Sun, H. Zeng, *J. Am. Chem. Soc.* **2002**, *124*, 8204.
[10] S. Peng, Y. Lee, C. Wang, H. Yin, S. Dai, S. Sun, *Nano Res.* **2008**, *1*, 229.
[11] V. Mazumder, S. Sun, *J. Am. Chem. Soc.* **2009**, *131*, 4588.
[12] S. Maksimuk, S. Yang, Z. Peng, H. Yang, *J. Am. Chem. Soc.* **2007**, *129*, 8684.
[13] N. Zheng, J. Fan, G. D. Stucky, *J. Am. Chem. Soc.* **2006**, *128*, 6550.
[14] J. Chen, B. J. Wiley, Y. Xia, *Langmuir* **2007**, *23*, 4120.
[15] X. Huang, N. Zheng, *J. Am. Chem. Soc.* **2009**, *131*, 4602.
[16] Y. Piao, J. Kim, H. B. Na, D. Kim, J. S. Baek, M. K. Ko, J. H. Lee, M. Shokouhimehr, T. Hyeon, *Nat. Mater.* **2008**, *7*, 242.
[17] H. T. Zhu, J. Luo, J. K. Liang, G. H. Rao, J. B. Li, J. Y. Zhang, Z. M. Du, *Phys. B* **2008**, *403*, 3141.
[18] G. Narsinga Rao, Y. D. Yao, J. W. Chen, *IEEE Trans. Magn.* **2005**, *41*, 3409.
[19] R. D. Zysler, E. Winkler, M. Vasquez Mansilla, D. Fiorani, *Phys. B* **2006**, *384*, 277.
[20] Y. Y. Xu, X. F. Rui, Y. Y. Fu, H. Zhang, *Chem. Phys. Lett.* **2005**, *410*, 36.
[21] L. Néel in *Low Temperature Physics*, (Eds: C, Dewitt, B, Dreyfus, P. D. de Gennes), Gordon and Beach, New York **1962**, p. 413.

300 °C at a heating rate of 2 °C min^{-1} and kept at this temperature for 4 h. The solution was cooled down to room temperature. The Fe_3BO_5 nanorods were precipitated by adding 20 mL ethanol and centrifuged at 6 000 rpm for 6 min. The precipitate was redispersed in 15 mL hexane, and 20 mL ethanol was added to precipitate the Fe_3BO_5 nanorods again. To remove spherical Fe_3O_4 nanoparticles, the centrifugation speed was reduced to 3 500 rpm. The precipitate was purified once again with 15 mL hexane and 20 mL ethanol at a centrifugation speed of 3 500 rpm. The as-synthesized Fe_3BO_5 nanorods were dispersed in hexane.

Synthesis of Silica-Coated Nanorods: 8 mg of Fe_3BO_5 nanorods was dried from its hexane dispersion and then redispersed in 10 mL cyclohexane. In a flask, 1 mL IGEPAL CO-520 was dissolved in 15 mL cyclohexane. The nanorod cyclohexane dispersion was added slowly into IGEPAL CO-520 cyclohexane solution under magnetic stirring. The solution was stirred for an extra 30 min followed by subsequent injection of 300 μL ammonium hydroxide (28–30 wt%) and of 200 μL tetraethyl orthosilicate.

Final page numbers not assigned